Effect of off-stoichiometry and site disorder on the properties of Ni_3Al: II. Magnetics

2008 J. Phys.: Condens. Matter 20 445228

(http://iopscience.iop.org/0953-8984/20/44/445228)

J. Phys.: Condens. Matter **20** (2008) 445228 (12pp) doi:10.1088/0953-8984/20/44/445228

Effect of off-stoichiometry and site disorder on the properties of Ni_3Al: II. Magnetics

A C Abhyankar, A Semwal and S N Kaul[1]

School of Physics, University of Hyderabad, Central University PO, Hyderabad 500046, Andhra Pradesh, India

E-mail: kaul.sn@gmail.com

Received 1 April 2008, in final form 2 August 2008
Published 10 October 2008
Online at stacks.iop.org/JPhysCM/20/445228

Abstract

A detailed comparison between the magnetic behaviours of the 'as-prepared' ap-Ni_xAl_{100-x} alloys with $x = 74.3$, 74.8, 75.1 and 76.1 at.% (that have both compositional disorder and site disorder) and 'annealed' counterparts (that have only compositional disorder) over a wide range of temperatures and magnetic fields (H) permits us to draw the following conclusions about the role of disorder. Regardless of the type of disorder, Curie temperature, T_C, and spontaneous magnetization at 0 K, M_0, decrease in accordance with the power laws $T_C(x) = t_x(x - x_c)^\tau$ and $M_0(x) = m_x(x - x_c)^\psi$ as $x \to x_c$ (the threshold Ni concentration below which the long-range ferromagnetic order ceases to exist). Site disorder lowers the value of x_c by nearly 1 at.% Ni, enhances T_C for a given composition (more so as $x \to x_c$) by increasing the number of Ni nearest neighbours for a given Ni atom, and leaves M_0 essentially unaltered because site disorder has essentially no effect on the density of states, $N(E_F)$, at the Fermi level, E_F, and the shape of the density-of-states curve near E_F (except for $x \approx x_c$, where site disorder tends to primarily enhance $N(E_F)$ and thereby stabilize long-range ferromagnetic order for Ni concentrations below the threshold concentration, $x_c \cong 74.6$ at.%, dictated by compositional disorder). At low and intermediate temperatures, spontaneous magnetization, $M(T, H = 0)$, as well as the 'in-field' magnetization, $M(T, H)$, exhibit *non-Fermi liquid* behaviour in the samples ap-$Ni_{74.3}$ and ap-$Ni_{74.8}$. As x_c is approached from above, i.e. as the *compositional disorder* increases, *stronger deviations* from the Fermi liquid behaviour occur and the temperature range over which the *non-Fermi liquid behaviour* persists *widens*. In contrast, the ap-$Ni_{75.1}$ and ap-$Ni_{76.1}$ alloys follow the behaviour that the self-consistent spin-fluctuation theory predicts for a weak itinerant-electron ferromagnet with no disorder. Both compositional disorder and site disorder have no effect on the critical behaviour of the alloys near the ferromagnetic-to-paramagnetic phase transition.

1. Introduction

A recent appraisal [1] of the previously reported [2–9] results on the magnetic behaviour of binary Ni_xAl_{100-x} alloys with 73.5 at.% $\leqslant x \leqslant$ 76.5 at.% highlighted the controversies that surround the nature of magnetism in this weakly ferromagnetic alloy system. Attributing the disagreement between the results of earlier investigations to a complex interplay between the compositional disorder and site disorder, and to a complete neglect of the spin-wave contribution to magnetization at low temperatures, Kaul and Semwal made an attempt to unravel the individual roles of compositional disorder [1] and site disorder [10, 11]. To this end, the study of magnetization in the 'as-prepared' Ni_xAl_{100-x} alloys [1] with 74 at.% $\leqslant x \leqslant$ 76 at.% (the Ni concentration range that includes the critical concentration [2–7] $x_c \approx$ 74.5 at.% below which long-range ferromagnetic order ceases to exist) and in the alloy of stoichiometric composition, Ni_3Al, 'prepared' in different states of site disorder [10, 11],

[1] Author to whom any correspondence should be addressed.

revealed the following. (i) Regardless of the degree of site disorder present, spin waves at low temperatures ($0.09T_C \leqslant T \leqslant 0.28T_C$), zero-point and thermally excited local spin-density fluctuations at intermediate temperatures ($0.32T_C \leqslant T \leqslant 0.62T_C$), and non-propagating thermally excited spin fluctuations at temperatures close to the Curie point, T_C ($0.65T_C \leqslant T \leqslant 0.95T_C$), completely account for [10, 11] the thermal demagnetization of spontaneous magnetization, $M(T, 0)$, and 'in-field' magnetization, $M(T, H)$. In contrast, the spin-fluctuation theories [12–14], that predict precisely this behaviour of $M(T, 0)$ and $M(T, H)$ for a weak itinerant-electron ferromagnet *in the absence of any disorder*, failed [1] to describe the decline in $M(T, H = 1\ \text{kOe})$ with increasing temperature observed in the Ni_xAl_{100-x} alloys that have substantial compositional disorder. Instead, the functional form of $M(T, H = 1\ \text{kOe})$ observed in these alloys could be closely reproduced over the entire temperature range, $T \leqslant T_C$, by the temperature variation predicted by the percolation (*localized-spin*) theories [15–17] that invoke a crossover in the spin dynamics on a three-dimensional ferromagnetic percolating network from a hydrodynamic (magnon) regime at low temperatures to a critical (fracton) regime at high temperatures. Moreover, the power laws, $M_0(x) \sim (x - x_c)^{\beta_P}$, $D_0(x) \sim (x - x_c)^{\theta_P}$ and $T_C(x) \sim (x - x_c)^{\phi}$ with $x > x_c$, which, according to the percolation theories [15, 16], characterize the percolation critical behaviour (second-order phase transition) at $x = x_c$ in three-dimensional percolating networks, described very well the Ni concentration dependences of the spontaneous magnetization at 0 K, $M_0 \equiv M(0, 0)$, the spin-wave stiffness at 0 K, D_0, and the Curie temperature, T_C. (ii) Like compositional disorder, site disorder smears out the sharp features in the density-of-states (DOS) curve near the Fermi level, E_F, and reduces the DOS at E_F, $N(E_F)$, M_0, D_0 and T_C. (iii) Site disorder affects the magnitude of suppression of the low-lying magnetic excitations (spin waves and spin fluctuations) by external magnetic field (H) but does not alter the functional form of the suppression with H.

Though the above observations (i)–(iii) facilitated characterizing the roles of site disorder and compositional disorder in influencing the magnetic properties of the weakly ferromagnetic alloy system, Ni_xAl_{100-x}, they concomitantly raised the following basic questions. (1) Why do the spin-fluctuation theories [12–14], which otherwise enjoy the distinction of providing a correct explanation for the characteristic attributes of weak itinerant-electron magnets, fail to describe the magnetic behaviour of weak itinerant-electron ferromagnets with compositional disorder? (2) How does one reconcile to the fact that weak *itinerant-electron* ferromagnets with compositional disorder follow closely the predictions of a *localized-spin* (percolation) theory? As a reconciliatory measure, Kaul and Semwal [1] conjectured that quenched random disorder in such systems could cause localization of the otherwise itinerant magnetic moments. This conjecture, however, does not explain as to why site disorder cannot be as effective in localizing the magnetic moments as compositional disorder supposedly is. The non-Fermi liquid behaviour of resistivity at low temperatures in the same alloy system, Ni_xAl_{100-x}, reported in the preceding paper [18] (henceforth referred to as paper I), adds a new dimension to the problem.

To seek answers to these fundamental queries, extensive high-resolution bulk magnetization, $M(T, H)$, measurements were undertaken on well-characterized samples of Ni_xAl_{100-x} alloys, in the 'as-prepared' state. An elaborate analysis of the present $M(T, H)$ data not only resolves issues (1) and (2), mentioned above, by bringing out clearly the effect of compositional disorder and/or site disorder on the contributions to $M(T, 0)$ and $M(T, H)$, arising from spin waves at low temperatures and non-propagating thermally excited longitudinal and transverse spin fluctuations at intermediate temperatures and for temperatures close to T_C, but also quantifies the suppression of these contributions by H. At low temperatures, $M(T, 0)$ and $M(T, H)$ exhibit non-Fermi liquid behaviour in the alloys with $x_c \cong 73.5$ at.% $\leqslant x < 75.1$ at.%, much the same way as the resistivity and magnetoresistance do, as reported in paper I. The present results also demonstrate that the compositional disorder and site disorder (for a precise definition of the terms 'compositional disorder' and 'site disorder', see section 2.2 of paper I) change T_C drastically but have practically no effect on the magnetic behaviour in the critical region since, irrespective of the amount or type of disorder present, mean-field critical exponents characterize the ferromagnetic-to-paramagnetic phase transition at T_C.

2. Experimental details

For magnetic measurements, spherically shaped samples (2.5 mm in diameter) of ap-$Ni_{74.3}$, ap-$Ni_{74.8}$, ap-$Ni_{75.1}$ and ap-$Ni_{76.1}$ were spark-cut from the 'as-prepared' (ap) rods, as already mentioned in paper I. Note that the magnetization, resistivity and magnetoresistance samples come from the *same* batch. Though the composition of these alloys is not very different from those used previously in [1], the x-ray diffraction patterns of the corresponding compositions are distinctly different (cf figure 1 of paper I with figure 1 of [1]) in that the substantial (200) texture, present in the earlier samples, is completely absent in the new ones.

Magnetization, $M(T, H_{ext})$, of polycrystalline Ni_xAl_{100-x} samples was measured in external static magnetic fields (H_{ext}) up to 15 kOe on a vibrating sample magnetometer (VSM). These measurements cover a temperature range of 15 K $\leqslant T \leqslant$ 300 K that embraces the critical region near the ferromagnetic (FM)–paramagnetic (PM) phase transition. M versus H_{ext} isotherms were taken at 60 predetermined but fixed values of H_{ext} (each stable to within ± 1 Oe) ranging from 0 to 15 kOe, at the temperature intervals of 0.5, 0.1, 0.05 and 0.025 K within the ranges 15 K $\leqslant T \leqslant 0.5T_C$, $0.5T_C \leqslant T \leqslant T_C - 10$ K, $T_C - 10$ K $\leqslant T \leqslant T_C - 3$ K, $T_C - 3$ K $\leqslant T \leqslant T_C + 3$ K and then the temperature interval was slowly increased to 0.1, 0.5, 1, 5 and 10 K while increasing the temperature to 300 K. A demagnetizing factor, N, was computed from the inverse slope of the linear M–H_{ext} isotherm (i.e. $4\pi N = (\text{slope})^{-1} = H_{ext}/M$) taken at the lowest temperature $T = 15$ K in the field range -20 Oe $\leqslant H_{ext} \leqslant 20$ Oe. To construct the Arrott ($M^2(T, H)$ versus $H/M(T, H)$) plots out of the $M(T, H_{ext})$ data, the external magnetic field was corrected for the demagnetizing

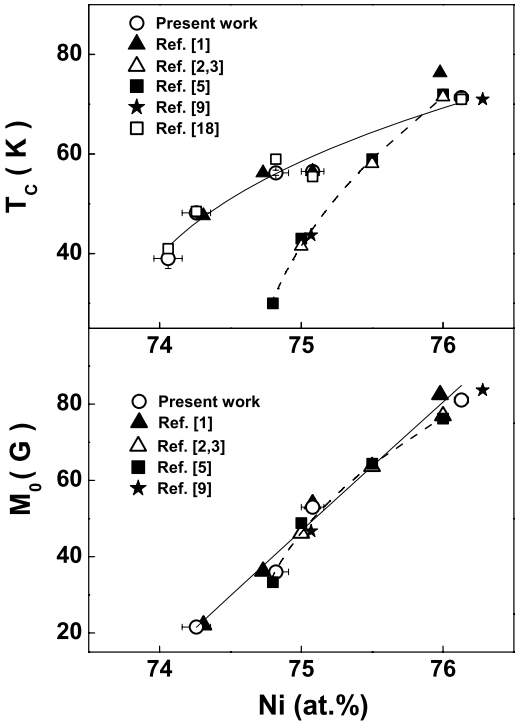

Figure 1. Variations of T_C and M_0 with Ni concentration, x, compiled from the values of T_C and M_0 obtained in the present work and those reported previously on the alloys with the same or similar composition. Continuous (dashed) curves represent the best least-squares fits to our (those reported in [2, 3, 5] and [9]) $T_C(x)$ and $M_0(x)$ data based on the power laws mentioned in the text.

field, i.e. $H = H_{ext} - 4\pi NM(T, H_{ext})$. The spontaneous magnetization at different temperatures, $M(T, H = 0)$, was computed from the intercepts on the ordinate obtained by extrapolating the high-field (also the low-field) portion of the Arrott plot isotherms to $H = 0$ (in the case of ap-$Ni_{74.3}$) for $T \leqslant T_C$, as elucidated in section 3.4. The M–H isotherms, used for constructing Arrott plots, were converted into the M–T data at 16 different but fixed values of H in the interval 0.3 kOe $< H <$ 15 kOe. Note that the above-mentioned detailed magnetization measurements were not performed on the ap-$Ni_{75.1}$ sample when the preliminary measurements revealed a magnetic behaviour that was not significantly different from the one reported earlier [10, 11] on the annealed counterpart of this sample. However, magnetization was measured on all the samples, including ap-$Ni_{75.1}$, as a function of H_{ext} for $H_{ext} \leqslant 70$ kOe at $T = 5$ K (and at a few specific temperatures so that a quantitative comparison between the magnetoresistance data and the spin-fluctuation theory could be made in paper I) and as a function of temperature in the range from 5 to 150 K at $H_{ext} = 1$ kOe, using a SQUID magnetometer.

3. Results and discussion

The Curie temperature, T_C, and spontaneous magnetization at 0 K, $M_0 \equiv M(0, 0)$, determined from the Arrott plots by the following procedure, are displayed in the top and bottom panels of figure 1. While T_C corresponds to the temperature at which the *linear* Arrott plot isotherm passes through the origin, M_0 is computed from the intercept on the ordinate yielded by a linear extrapolation [1] of the high-field portion of the $M^2(T, H)$ versus $H/M(T, H)$ plot at $T = 5$ K to $H = 0$. Alternatively, M_0 is extracted from the optimum fit to the $M(T = 5\text{ K}, H)$ isotherm for fields above the technical saturation, i.e. over the range 2 kOe $\leqslant H \leqslant$ 70 kOe, based on the expression [1, 10] $M(T = 5\text{ K}, H) = M_0 + \lambda\sqrt{H} + \chi_{hf}H$, where the $\sqrt{H}$ term accounts for the suppression of spin waves by the field H [19] and the high-field susceptibility, χ_{hf}, is related to the exchange-enhanced Pauli spin susceptibility [1, 10]. Both the determinations yield the same value (within the uncertainty limits) for M_0 for a given composition. Figure 1 compares the values of T_C and M_0, so obtained for the samples ap-$Ni_{74.3}$, ap-$Ni_{74.8}$, ap-$Ni_{75.1}$ and ap-$Ni_{76.1}$, with those determined for the same samples (samples of similar composition) from resistivity and magnetoresistance [18] (in the literature [1–3, 5, 9]). Note that only the Ni atoms carry magnetic moment in the alloys in question and hence compositional and/or site disorder in the Ni sub-lattice alone is of direct relevance so far as the magnetic properties are concerned. Considering that the *'as-prepared' samples* used in the present magnetization, resistivity and magnetoresistance [18] measurements and in the previous study [1] have *both compositional disorder and site disorder* whereas the *well-annealed* (and hence completely ordered) *counterparts* used in earlier investigations [2, 3, 5, 9] have *only compositional disorder*, the following unambiguous conclusions about the roles of compositional disorder and site disorder can be drawn from the comparison made in figure 1. (i) With increasing compositional disorder, i.e. as $x \to x_c$, T_C and M_0, in the alloys with compositional disorder alone, decrease in accordance with the power laws (dashed curves) $T_C(x) = t_x(x - x_c)^\tau$ and $M_0(x) = m_x(x - x_c)^\psi$ with $x_c = 74.60(6)$ at.%, $\tau = 0.43(5)$ and $\psi = 0.40(8)$. (ii) The effect of site disorder is to slow down the variations (continuous curves) of T_C and M_0 with x such that the above power laws still hold but with $x_c = 73.6(1)$ at.%, $\tau = 0.33(3)$ and $\psi = 1.00(5)$. Alternatively, compared to the values of T_C for the Ni_xAl_{100-x} alloys with compositional disorder alone, site disorder enhances T_C for a given composition (leaves T_C essentially unaltered) and this enhancement grows rapidly as $x \to x_c$ (for $x \geqslant 76$ at.%). In sharp contrast with this behaviour, except for $x \approx x_c$, M_0 is relatively *insensitive* to site disorder. Why $T_C(x)$ is more sensitive to site disorder than $M_0(x)$ can be understood [1, 10] as follows, in terms of the spin-fluctuation theories [12–14] that yield the expressions for T_C and M_0:

$$T_C = \left(\frac{2\pi^2}{5\alpha}\right)^{3/4}\left(\frac{c_\nu}{k_B}\right)(\hbar\gamma_\nu)^{1/4}M_0^{3/2} \quad (1)$$

$$M_0 = N\mu_B 2^{1/2}\left\{[N'(E_F)]^2 - [N''(E_F)N(E_F)/3]\right\}^{-1/2} \times [N(E_F)]^2[IN(E_F) - 1]^{1/2}. \quad (2)$$

In equations (1) and (2), the coefficient of the gradient term in the Ginzburg–Landau expansion, c_ν, is a measure of the spin-fluctuation stiffness, while γ_ν and the quantity within the curly

brackets in equation (2) depend on the shape of the density-of-states (DOS) curve near the Fermi level, E_F, as well as on the DOS at E_F, $N(E_F)$. According to these expressions, M_0 is sensitive to both $N(E_F)$ and the shape of the DOS curve near E_F whereas, apart from these factors, T_C also depends on c_v. Thus, the insensitivity of M_0 to site disorder implies that site disorder has essentially no effect on $N(E_F)$ and the shape of the DOS curve near E_F (except for $x \approx x_c$, where site disorder tends to primarily enhance $N(E_F)$ and thereby stabilize long-range ferromagnetic order for Ni concentrations below the threshold concentration, $x_c \cong 74.6$ at.%, dictated by compositional disorder). It immediately follows that, as $x \to x_c$, site disorder increases the concentration of Ni atoms on the Al sub-lattice beyond that allowed by the compositional disorder and thereby enhances c_v (and hence T_C) because of the increase in the number of Ni nearest neighbours for a given Ni atom. Site disorder thus lowers the critical concentration, x_c, by nearly 1 at.% Ni.

Having discussed the influence of compositional disorder and site disorder on M_0 and T_C, we now focus our attention on their effect on the temperature and magnetic field dependences of magnetization in the temperature regimes where different kinds of low-lying magnetic excitations dominantly contribute to $M(T, H)$.

3.1. Low temperatures ($T \ll T_C$)

In weak itinerant-electron ferromagnets without any disorder, spin-wave modes of wavevector q, in the region around $q = 0$ in the Brillouin zone, exist as well-defined excitations at low temperatures, $T \ll T_C$. According to the spin-fluctuation theory [14], this spin-wave (SW) contribution to magnetization is given by

$$[M(T,0)]_{SW} = M(0,0) - g\mu_B\xi(3/2)[k_BT/4\pi D(T,0)]^{3/2}, \quad H = 0 \tag{3a}$$

$$[M(T,H)]_{SW} = M(0,H) - g\mu_B Z(3/2,t_H) \times [k_BT/4\pi D(T,H)]^{3/2}, \qquad H \neq 0. \tag{3b}$$

In these equations, the Bose function $Z(3/2, t_H) = \sum_{n=0}^{\infty} n^{-3/2}e^{-nt_H}$ with the reduced field $t_H = g\mu_B H/k_BT$ allows for the energy gap in the spin-wave spectrum, introduced by H_{ext} and anisotropy fields, and D is the spin-wave stiffness. In the case of weak itinerant-electron ferromagnets, D renormalizes with temperature as $D(T) = D(0)(1 - D_2T^2)$ where the spin-wave stiffness at 0 K, $D_0 \equiv D(0) = g\mu_B c_\perp M(0,0)$, is independent of the field. An attempt has been made to determine D_0, the thermal-renormalization coefficient, D_2, $M_0 \equiv M(0,0)$ and 'in-field' magnetization at 0 K, $M(0,H)$, from the fits to the $M(T,0)$ and $M(T,H)$ data based on equations (3*a*) and (3*b*), respectively, using the 'range-of-fit' analysis in which the variation in the above-mentioned parameters is monitored as the temperature range ($T \ll T_C$) of the fit is varied. Due to the extra temperature variations introduced by the thermal renormalization of spin-wave stiffness and the presence of the function $Z(3/2, t_H)$ in equation (3*b*), equations (3*a*) and (3*b*) predict a *concave-downward* curvature in the $M(T,0)$ versus $T^{3/2}$ and $M(T,H)$ versus $T^{3/2}$ plots. In sharp contradiction with this prediction, the $M(T, H = 1$ kOe) versus $T^{3/2}$ plots for ap-$Ni_{74.3}$ and ap-$Ni_{74.8}$ alloys, shown in the inset of figure 2(a), exhibit a *concave-upward* curvature, which is more pronounced in the alloy ap-$Ni_{74.3}$ whose composition is closer to the critical concentration $x_c \cong 73.6$ at.%. Exactly the same behaviour was observed previously [1] in the alloys of similar composition. Thus, equations (3*a*) and (3*b*) cannot describe the temperature dependence of magnetization in the alloys ap-$Ni_{74.3}$ and ap-$Ni_{74.8}$. In contrast, the $M(T, H = 1$ kOe) versus $T^{3/2}$ plots for the ap-$Ni_{75.1}$ and ap-$Ni_{76.1}$ alloys, displayed in the inset of figure 2(b), show the expected curvature and equation (4) does indeed closely reproduce (continuous curves through the data points, represented by symbols) the observed $M(T)$ at 1 kOe, as is evident from the lower panel of figure 2(b). The percentage deviations of the data from the best least-squares (LS) fits based on equation (4), shown in the bottom panel of figure 2(b), do not exceed ± 0.02 in the temperature range 5 K $\leqslant T \leqslant$ 18 K. These LS fits yield the values for D_0 as 67.5(6) meV Å^2 and 70(1) meV Å^2 for the alloys ap-$Ni_{75.1}$ and ap-$Ni_{76.1}$, respectively. Lower magnitude of D_0 in 'as-prepared' $Ni_{75.1}$ ($Ni_{76.1}$) compared to $D_0 = 69.6(14)$ meV Å^2, from the magnetization data [10, 11] or $D_0 = 85(15)$ meV Å^2 ($D_0 = 95(5)$ meV Å^2), from inelastic neutron scattering results [20] ([21]), for a well-annealed, and hence completely ordered, counterpart, basically reflects a reduction in the coefficient $c_\perp$ by site disorder. That this is indeed the case is obvious from the relation $D_0 = g\mu_B c_\perp M_0$ and our observation that site disorder has essentially no effect on M_0 in this concentration range (figure 1).

The deviation plots, shown in the lower panel of figure 2(a), clearly demonstrate that the functional form

$$M(T,H) = M(0,H)\left(1 - A_n(H)T^n\right) \tag{4}$$

with $n = 1.20(1)$ and 1.25(1) describes the $M(T, H = 1$ kOe) data in the temperature ranges 5 K $\leqslant T \leqslant$ 25 K and 5 K $\leqslant T \leqslant$ 20 K for the samples ap-$Ni_{74.3}$ and ap-$Ni_{74.8}$ far better than either equation (3*b*) or other forms $M \sim T^2$ [2, 3, 5] and $M^2 \sim T^2$ [6, 7] used in the literature for completely ordered samples. Spin-fluctuation theories [22, 23] of non-Fermi liquid behaviour, which do not include any kind of disorder, predict $n = 4/3$ for a three-dimensional weak itinerant-electron ferromagnet. The finding that the values of the exponent n for the samples ap-$Ni_{74.3}$ and ap-$Ni_{74.8}$ are closer to this value (1.33) than $n = 1.5$, expected for the normal spin-wave behaviour at low temperatures, asserts that these samples, with composition close to the critical concentration $x_c = 73.6(1)$ at.%, exhibit non-Fermi liquid behaviour. This inference is not only consistent with the similar behaviour observed in the resistivity [18] (specific heat [8]) of these samples (the samples with similar composition) in nearly the same temperature ranges but also with the premise that the non-Fermi liquid behaviour for $x \approx x_c$ is a consequence of the alteration in the spin-wave dispersion, leading to severe damping of spin waves, brought about primarily by compositional disorder (with site disorder only tending to enhance the effect of compositional disorder); for details, see the paragraph following equation (7) in paper I.

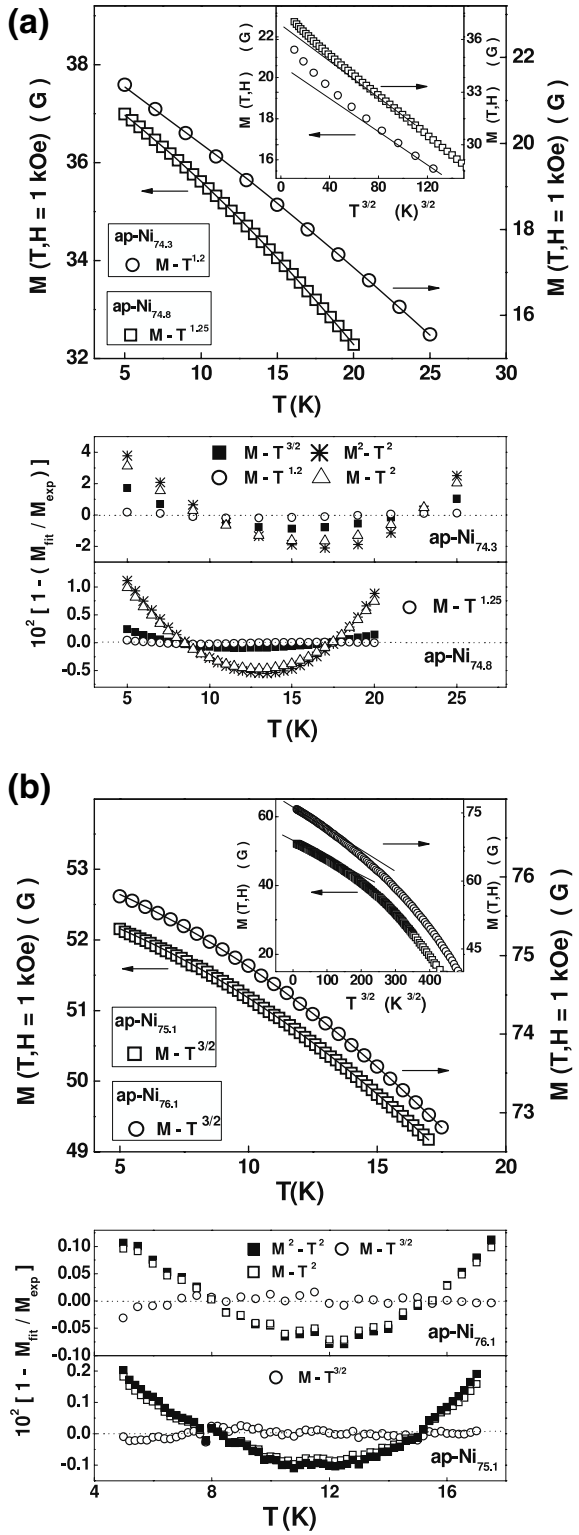

Figure 2. The upper panels display $M(T, H = 1\ \text{kOe})$ as a function of temperature at low temperatures for the samples ap-$Ni_{74.3}$, ap-$Ni_{74.8}$, ap-$Ni_{75.1}$ and ap-$Ni_{76.1}$ along with the best least-squares fits (continuous curves) through the data (open circles) based on equations (3*b*) and (4) of the text, while the lower panels show the corresponding percentage deviations of the data from the fits based not only on equations (3*b*) and (4) but also on the other expressions used previously in the literature. The inset in the upper panel of figure 2(a) serves to highlight the concave-upward deviations of the $M(T, H = 1\ \text{kOe})$ data from the spin-wave $T^{3/2}$ law in the case of the samples ap-$Ni_{74.3}$ and ap-$Ni_{74.8}$.

The suppression of spin waves or over-damped spin waves by the external magnetic field can be quantified by monitoring the field dependence of either the coefficient, $A_{3/2}$, of the $T^{3/2}$ term when equation (3*b*) is cast in the form of equation (4) or the coefficient A_n in equation (4). The coefficients $A_n(H)$ with $n = 1.2$, 1.25 or 1.5 are nothing other than the slopes of the *linear* M–T^n plots, for a given value of n, at fixed values of H, as illustrated by figure 3(a). The representative data shown in figure 3(a) highlight that the exponent n does not depend on H while the linear A_n–$\sqrt{H}$ plots in figure 3(b) demonstrate that the coefficient A_n of the T^n term decreases with increasing H in accordance with the relation [19]

$$A_n(H) = A_n(0)\left(1 - \nu H^{1/2}\right). \tag{5}$$

The spin-fluctuation theory [19] thus correctly predicts a *field-independent* exponent n and the $\sqrt{H}$ suppression of spin waves with magnetic field. For a given composition, the value of $A_n(0) \equiv A_n(H = 0)$, obtained by extrapolating the linear $A_n(H) - \sqrt{H}$ plot (the least-squares fit straight lines shown in figure 3(b)) to $H = 0$, exactly coincides with that (solid symbol) determined directly from the slope of the linear spontaneous magnetization, $M(T, H = 0)$, versus T^n plot (e.g. the straight line through the data points denoted in figure 3(a) by crosses). Figure 4 displays the variations of $A_n(H = 0)$ and ν with the Ni concentration, x. While $[A_n(H = 0)]^{-1}$ is a measure of spin-wave stiffness (cf equations (3*a*) and (4)), the coefficient ν of the $\sqrt{H}$ term quantifies the suppression of spin waves by H. Thus, the observed increase in $A_n(H = 0)$ as $x \to x_c$ implies that the compositional disorder lowers the thermal energy required to excite long-wavelength spin waves. Similarly, the observed variation of ν with x conveys that the compositional disorder promotes the field-induced suppression of spin waves by reducing their stiffness.

3.2. *Intermediate temperatures ($T < T_C$)*

In the intermediate range of temperatures, the spin-wave contribution to $M(T, 0)$ and $M(T, H)$ is completely masked by that arising from non-propagating spin fluctuations (SF). The self-consistent spin-fluctuation calculations [14] yield the following expression for the spin-fluctuation contribution to magnetization at intermediate temperatures

$$[M(T, H)]_{\text{SF}} = M(0, H)[1 - A_2(H)T^2 - A_{4/3}T^{4/3}]^{1/2}, \tag{6}$$

which is valid for both $H = 0$ and $H \neq 0$. In equation (6), the T^2 term is solely due to the thermally excited (TE) spin fluctuations while the $T^{4/3}$ term is the net result of the competing claims [14] made by TE and zero-point (ZP) components of spin fluctuations with ZP contribution dominating over the TE one. The TE contribution gets progressively suppressed by H whereas the ZP contribution is nearly independent of H. The 'range-of-fit' analysis of the $M(T, H = 1\ \text{kOe})$ data based on equation (6) yielded different results for different compositions (figure 5). Since the contribution of spin waves to magnetization persists to temperatures well above $0.5T_C$ in ap-$Ni_{74.3}$, an extremely

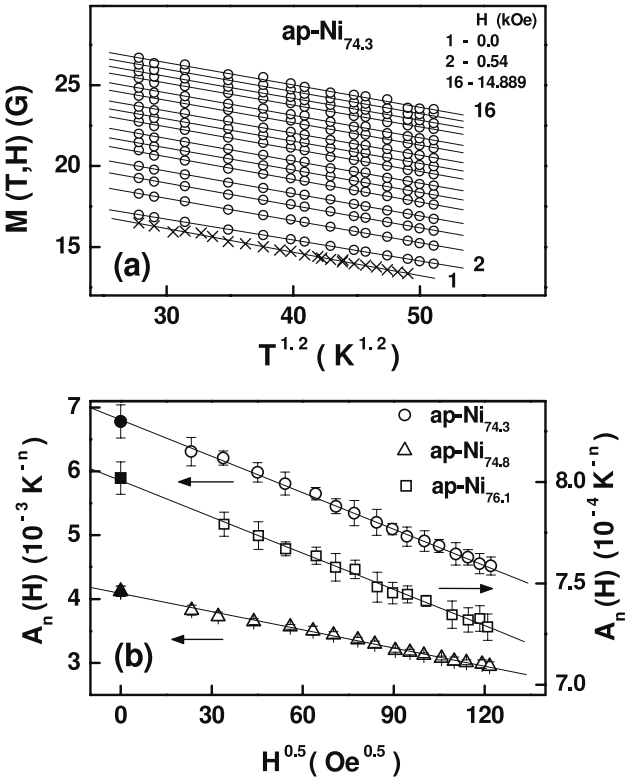

Figure 3. The upper panel displays a typical low-temperature M–T^n plot at a few representative but fixed values of H. The continuous lines through the $M(T, H)$ data (open circles) and $M(T, H = 0)$ data (crosses) are the least-squares fits based on equation (5). The lower panel demonstrates that the coefficient A_n of the T^n term (with $n = 1.2$, 1.25 and 1.5 for the samples ap-$Ni_{74.3}$, ap-$Ni_{74.8}$ and ap-$Ni_{76.1}$, respectively) in equation (4) varies linearly with $\sqrt{H}$ and thereby testifies to the validity of equation (5).

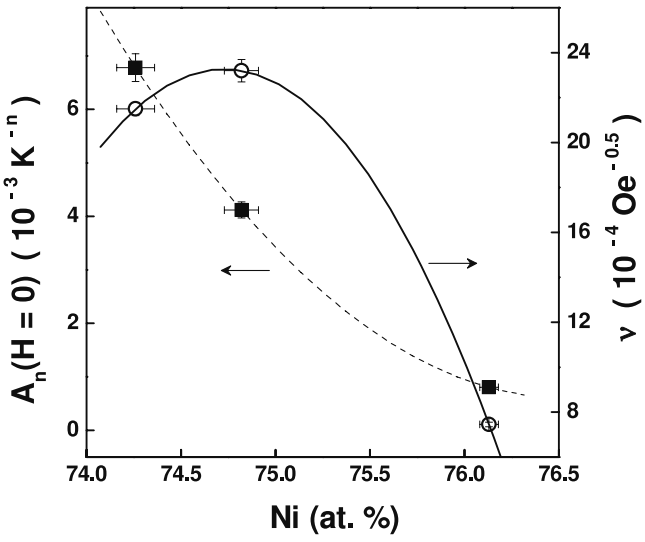

Figure 4. Variations of the prefactor $A_n(0) \equiv A_n(H = 0)$ and the coefficient ν (appearing in equation (5)) with Ni concentration. Smooth curves through the data serve only as a guide to the eye.

narrow intermediate temperature range precluded a meaningful comparison with theory [14], i.e. with equation (6). In the ap-$Ni_{74.8}$ sample, the T^2 term is so small that $[M(T, H)]^2$

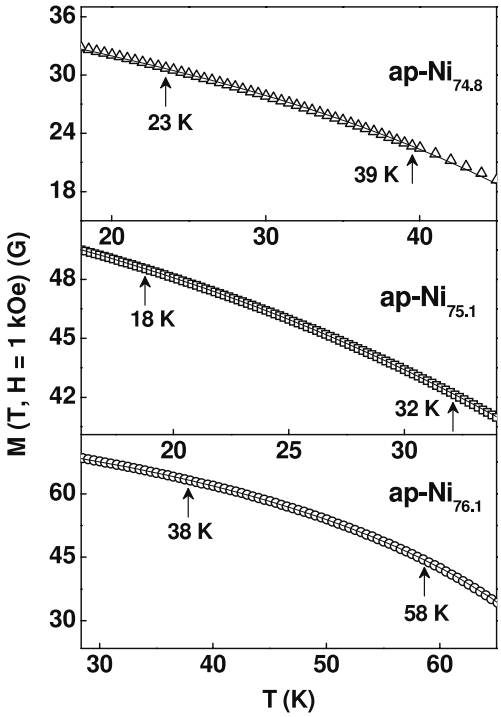

Figure 5. Temperature variations of $M(T, H = 1$ kOe) at intermediate temperatures for the samples ap-$Ni_{74.8}$, ap-$Ni_{75.1}$ and ap-$Ni_{76.1}$. The continuous curves through the data points (open symbols) represent the theoretical fits based on equation (6) of the text.

varies as $T^{4/3}$ (the upper panel in figure 6(a)) and contrary to the theoretical expectation [14] that the coefficient $A_{4/3}$ is independent of H (equation (6)), $A_{4/3}(H) \sim \sqrt{H}$ (see the lower panel of figure 6(a)). As we shall show in section 3.3, a total absence of the T^2 term and hence a complete dominance of the $T^{4/3}$ term, and the $\sqrt{H}$ variation of $A_{4/3}(H)$, mark the characteristic attributes of the spin-fluctuation contribution to $M(T, H)$ at temperatures close to T_C. In this context, at intermediate temperatures, ap-$Ni_{74.8}$ behaves as if it were near a quantum critical point. Thus, in concurrence with the conclusions drawn from the resistivity data [18], the non-Fermi liquid behaviour is observed over an unusually wide temperature range $T \leqslant 0.55T_C$ in ap-$Ni_{74.3}$ and ap-$Ni_{74.8}$. Contrasted with this behaviour, equation (6) completely accounts for (continuous curves through the data points) the observed temperature dependence of $M(T, H)$ (open squares or circles) and $M(T, H = 0)$ (crosses) in ap-$Ni_{75.1}$ and ap-$Ni_{76.1}$ over the temperature ranges $0.3T_C \leqslant T \leqslant 0.6T_C$ and $0.5T_C \leqslant T \leqslant 0.75T_C$, apparent in figure 5 and in the upper panel of figure 6(b). In conformity with the predictions of the self-consistent spin-fluctuation model [14], the coefficient $A_{4/3}$ of the $T^{4/3}$ term is *independent* of H whereas that of the T^2 term, A_2, depends *linearly* on H (the lower panel of figure 6(b)) and follows the relation $A_2(H) = A_2(0)(1 - \varphi H)$ with $A_2(0) = 1.45(2) \times 10^{-4}$ K^{-2} and $\varphi = 1.87(5) \times 10^{-5}$ Oe^{-1}. These values are *lower* than those $A_2(0) = 3.12(2) \times 10^{-4}$ K^{-2} and $\varphi = 2.12(13) \times 10^{-5}$ Oe^{-1} reported [10, 11] for the ordered Ni_3Al compound.

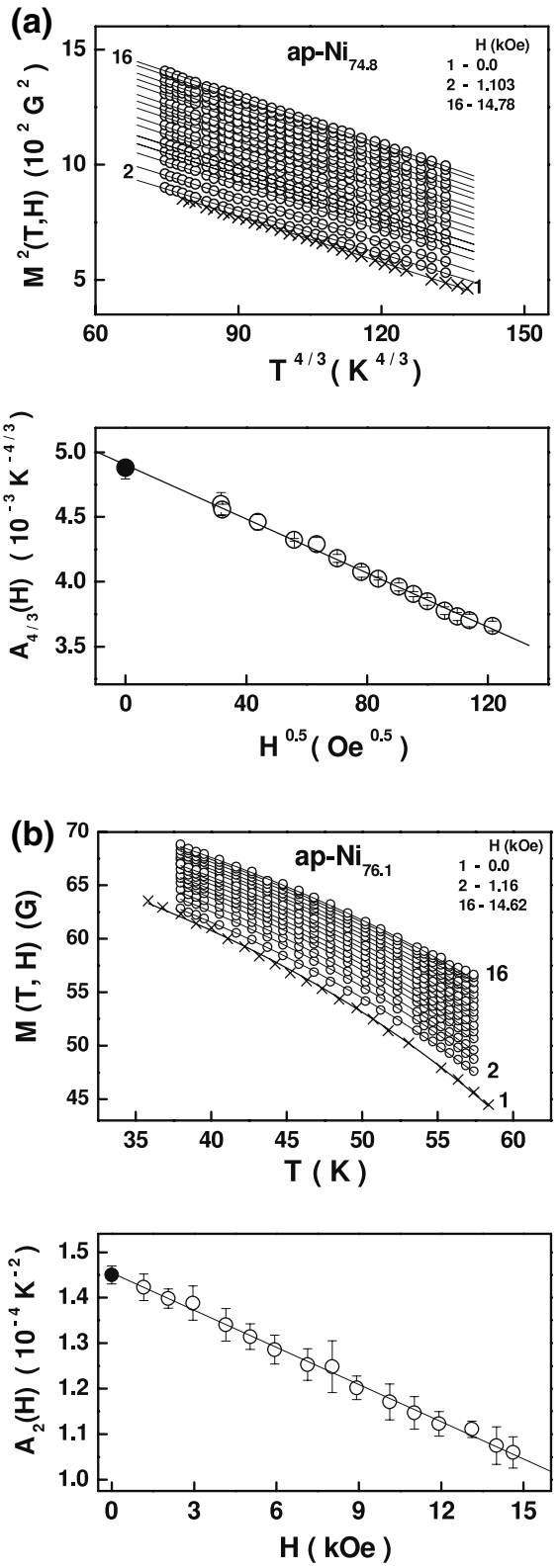

Figure 6. The upper panels display the M^2–$T^{4/3}$ and M–T plots at intermediate temperatures for a few representative but fixed values of H for the samples ap-$Ni_{74.8}$ and ap-$Ni_{76.1}$, respectively. The continuous lines through the $M(T, H)$ data (open circles) and $M(T, H = 0)$ data (crosses) are the least-squares fits based on equation (6). The lower panel in (a) ((b)) demonstrates that the coefficient $A_{4/3}(H)$ [$A_2(H)$] of the $T^{4/3}$ [T^2] term in equation (6) varies linearly with $\sqrt{H}$ [H].

Recognizing that [14] $[A_2(0)]^{-1}$ is a measure of the spin-fluctuation stiffness while the slope φ of the A_2 versus H straight line quantifies the suppression of thermally excited (TE) spin fluctuations by magnetic field, reduced values of $A_2(0)$ and φ in the sample ap-$Ni_{76.1}$ indicate that, with increasing Ni concentration, the TE spin fluctuations become more 'stiff' and hence the rate of their suppression with H also slows down.

3.3. Temperatures close to T_C

For temperatures close to T_C but outside the critical region, the self-consistent calculations [14] of the thermally excited (TE) and/or zero-point (ZP) spin-fluctuation contributions to magnetization, in the presence ($H \neq 0$) and absence ($H = 0$) of magnetic field, yield the expression

$$[M(T, H)]_{SF} = M(0, H)[1 - A_{4/3}(H)T^{4/3}]^{1/2} \qquad (7)$$

and make the specific prediction [14]

$$A_{4/3}(H) = A_{4/3}(H = 0)[1 - \eta H^{1/2}] \qquad (8)$$

about the functional form of the coefficient $A_{4/3}(H)$ of the $T^{4/3}$ term in equation (7). In equation (7), the $T^{4/3}$ term for $H = 0$ (or, equivalently, $A_{4/3}(H = 0)$) originates from both ZP and TE spin fluctuations whereas the same term in finite fields, i.e. $A_{4/3}(H \neq 0)$, arises from the TE spin fluctuations alone. An elaborate analysis of the $M(T, H)$ and $M(T, H = 0)$ data taken at temperatures close to T_C (typically in the temperature range $0.75T_C \leqslant T \leqslant 0.93T_C$) based on equation (7), along the lines already described in sections 3.1 and 3.2, allows us to make the following important observations. (i) That the observed functional forms of the 'in-field' magnetization, $M(T, H)$, and spontaneous magnetization, $M(T, H = 0)$, at such temperatures are best described by equation (7) is evident from the linear $M^2(T, H) - T^{4/3}$ (open circles) and $M^2(T, H = 0) - T^{4/3}$ (crosses) plots, shown in figures 7 and 8(a). (ii) Similarly, the linear variation of the coefficient $A_{4/3}(H)$ with $\sqrt{H}$ (figure 8(b)) conforms very well with the theoretical prediction [14], equation (8). Furthermore, a linear extrapolation of the $A_{4/3}(H) - \sqrt{H}$ plots to $H = 0$ always yields the same value (within the uncertainty limits) for $A_{4/3}(H = 0)$ as that directly determined (solid circle) from the slope of the linear $M^2(T, H = 0) - T^{4/3}$ plot. (iii) Both $A_{4/3}(H = 0)$ and η decrease with increasing Ni concentration, as shown in figure 9. The values $A_{4/3}(H = 0) = 4.65(3) \times 10^{-3}$ $K^{-4/3}$ and $\eta = 2.63(2) \times 10^{-3}$ $Oe^{-1/2}$, reported [10, 11] for the *ordered* Ni_3Al, included in figure 9 for comparison, are much higher than the 'as-prepared' site disordered counterpart.

Considering that both ZP and TE (only TE) spin fluctuations give rise to $A_{4/3}(H = 0)$ ($A_{4/3}(H \neq 0)$), $[A_{4/3}(H = 0)]^{-1}$ is a direct measure of the 'stiffness' of the ZP and TE spin fluctuations while the coefficient η in the expression, equation (8), for $A_{4/3}(H)$ *quantifies* the suppression of TE spin fluctuations by magnetic field. In view of this assignment, the above observation (iii) implies

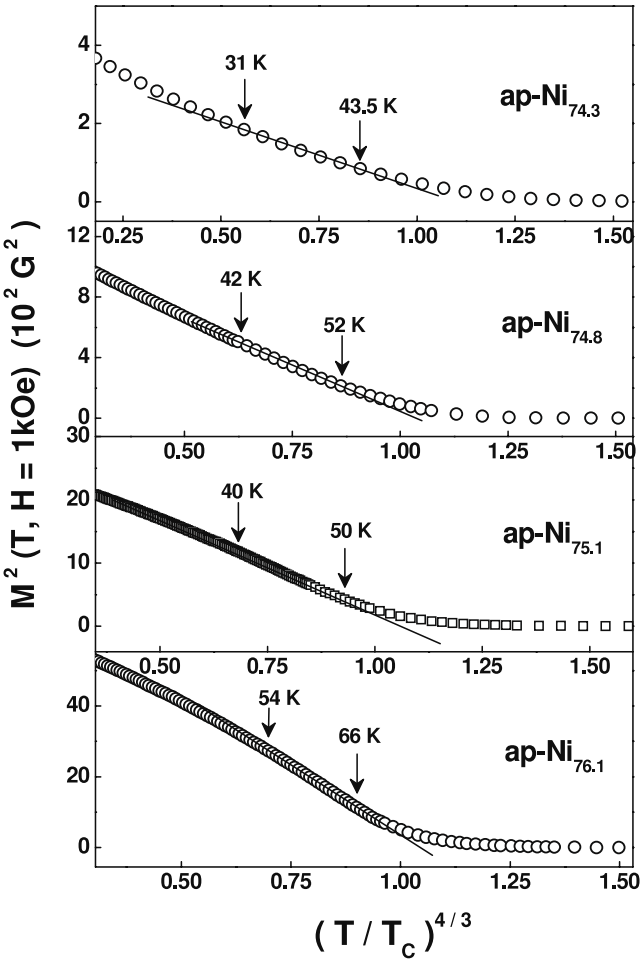

Figure 7. $M^2(T, H = 1$ kOe) as a function of $(T/T_C)^{4/3}$ at temperatures close to the Curie point, T_C, for the samples ap-$Ni_{74.3}$, ap-$Ni_{74.8}$, ap-$Ni_{75.1}$ and ap-$Ni_{76.1}$. The best least-squares fits (continuous curves) through the data (open symbols) are based on equation (7) of the text.

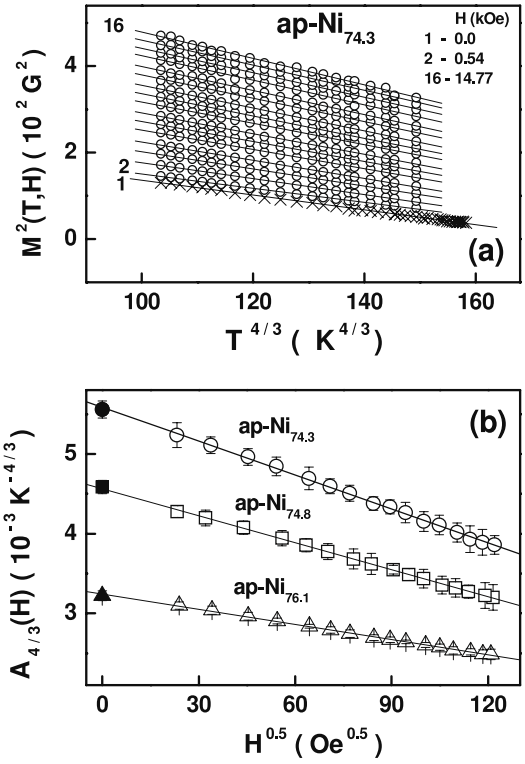

Figure 8. The upper panel displays the typical M^2–$T^{4/3}$ plots at temperatures close to T_C for a few representative but fixed values of H. The continuous lines through the $M^2(T, H)$ data (open circles) and $M^2(T, H = 0)$ data (crosses) are the least-squares fits based on equation (7). The lower panel demonstrates that the coefficient $A_{4/3}(H)$ of the $T^{4/3}$ term in equation (7) varies linearly with $\sqrt{H}$ for the samples ap-$Ni_{74.3}$, ap-$Ni_{74.8}$ and ap-$Ni_{76.1}$ and thereby testifies to the validity of equation (8).

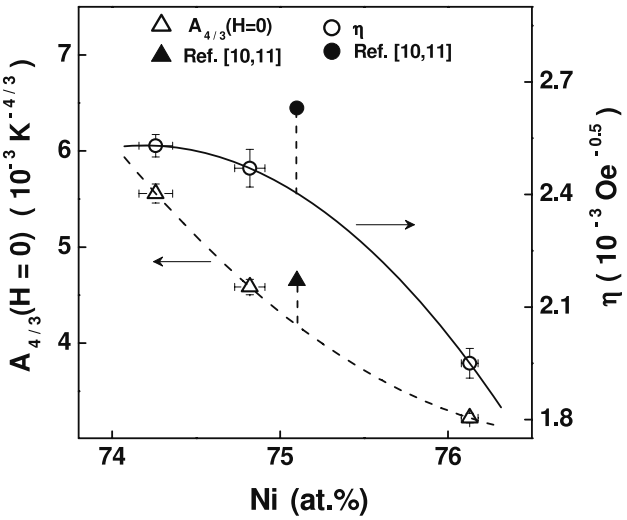

Figure 9. Variations of the prefactor $A_{4/3}(H = 0)$ and the coefficient η (appearing in equation (8)) with Ni concentration. The values for $A_{4/3}(H = 0)$ and η reported in [10, 11] for the stoichiometric composition are included for comparison. Smooth curves through the data serve only as a guide to the eye.

that increasing compositional disorder ($x \to x_c$) progressively lowers the 'stiffness' of the ZP and TE spin fluctuations so that the suppression of TE fluctuations, in particular, by field becomes correspondingly large (the ZP contribution is essentially independent of H [14]); site disorder also plays the same role so far as the stoichiometric composition is concerned. This inference becomes all the more evident when equation (8) is cast into the following scaling form:

$$[A_{4/3}(H)/A_{4/3}(H = 0)] = 1 - (H/H_0)^{1/2} \qquad (9)$$

where $H_0 = \eta^{-2}$ denotes the critical field at which the contribution to magnetization arising from the thermally excited spin fluctuations gets completely quenched. While figure 10 serves to demonstrate the validity of this scaling for the samples ap-$Ni_{74.3}$, ap-$Ni_{74.8}$ and ap-$Ni_{76.1}$, its inset shows that lower and lower fields are required to quench the TE spin-fluctuation contribution as the compositional disorder increases, i.e. as $x \to x_c$. The same decreasing trend in the fields required to quench the TE spin-fluctuation contribution to resistivity with the increasing degree of compositional disorder was observed in paper I but the values of H_0 were an order of magnitude higher. Another important aspect of the presently determined values of $A_{4/3}(H = 0)$ is that they yield the values for the Curie temperature $T_C^{SF} \cong 49.1, 56.8$

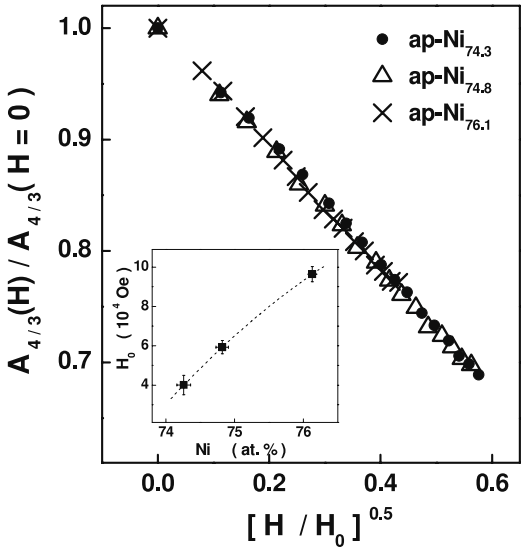

Figure 10. $A_{4/3}(H)/A_{4/3}(H=0)$ versus $(H/H_0)^{0.5}$ scaling plot for the samples ap-$Ni_{74.3}$, ap-$Ni_{74.8}$ and ap-$Ni_{76.1}$. The inset depicts the variation of the critical field H_0 (required to quench the spin-fluctuation contribution to magnetization at temperatures close to T_C) with the Ni concentration.

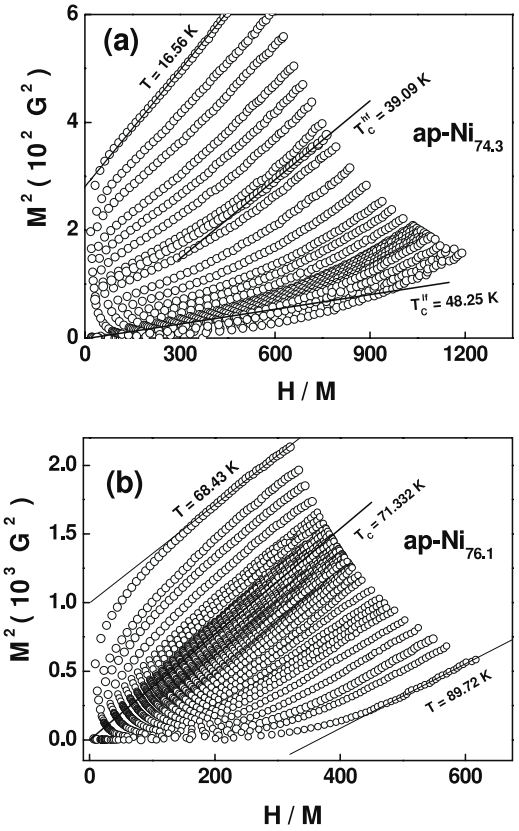

Figure 11. $M^2(T, H)$ versus $H/M(T, H)$ (Arrott) plots for samples (a) ap-$Ni_{74.3}$ and (b) ap-$Ni_{76.1}$ over a wide temperature range that embraces the critical region near the ferromagnetic-to-paramagnetic phase transition. These Arrott plots also indicate the values of T_C for the samples in question.

and 72.3 K for the samples ap-$Ni_{74.3}$, ap-$Ni_{74.8}$ and ap-$Ni_{76.1}$, respectively, when the relation [14] $T_C^{SF} = [A_{4/3}(H=0)]^{-3/4}$ is used. These values are fairly close to the actual values of T_C determined from the Arrott plots (figure 11).

At this stage, we return to the basic question as to why, in a previous report [1], the temperature dependence of magnetization at $H = 1$ kOe in the samples ap-$Ni_{74.31}$, ap-$Ni_{74.73}$ and ap-$Ni_{75.98}$ with composition similar to those used in this work, could be closely reproduced, over an unusually wide temperature range, $T \leqslant T_C$, by only the crossover percolation (*localized-spin*) theories but not by the spin-fluctuation (*itinerant-electron*) models. In the present case, the $M(T, H = 1$ kOe) data for the samples ap-$Ni_{74.3}$, ap-$Ni_{74.8}$, ap-$Ni_{75.1}$ and ap-$Ni_{76.1}$ could also be described very well by the crossover percolation theories with the values $T_{co}^* \cong 0.5$, 5, 20 and 40 K for the temperature T_{co}^* at which a crossover from the low-temperature magnon regime to high-temperature fracton regime occurs in a three-dimensional ferromagnetic percolating network. Note that these values of T_{co}^* agree quite well with those (table 2 in [1]) reported [1] previously for the similar alloy compositions. In view of this result, a spin-wave (*propagating transverse spin-fluctuation*) description of the temperature variations of the 'zero-field' (spontaneous) and 'in-field' magnetizations, within the framework of the localized-spin (spin-fluctuation) theories, is possible only for $T \leqslant T_{co}^*$. This inference is borne out by our finding that equations (3*a*) and (3*b*) correctly account for the decline in $M(T, 0)$ and $M(T, H)$ with increasing temperature observed in ap-$Ni_{75.1}$ and ap-$Ni_{76.1}$ for $T \leqslant 20$ K but fail to do so in ap-$Ni_{74.3}$ and ap-$Ni_{74.8}$ for 5 K $\leqslant T \ll T_C$ (figures 2 and 3), where these alloys with $x \approx x_c$ exhibit non-Fermi liquid behaviour. In hindsight, it now becomes apparent that the ferromagnetic fractons mimic the behaviour of over-damped spin waves and/or exchange-enhanced spin-density fluctuations at temperatures $T \geqslant T_{co}^*$.

3.4. Critical region

Figure 11 highlights the salient features of the Arrott ($M^2(T, H)$ versus $H/M(T, H)$) plots of the alloys with extreme compositions, i.e. ap-$Ni_{74.3}$ and ap-$Ni_{76.1}$, over a wide temperature range which embraces the critical region near the ferromagnetic (FM)–paramagnetic (PM) phase transition. It is customary [24] to compute spontaneous magnetization, $M(T, 0) \equiv M(T, H = 0)$, and inverse initial susceptibility, $\chi^{-1}(T)$, from the intercept values at different temperatures on the ordinate ($T \leqslant T_C$) and abscissa ($T \geqslant T_C$) obtained when the *linear high-field* portions of the Arrott plot (AP) isotherms are extrapolated to $H = 0$ and $M^2 = 0$, respectively, as shown in figure 11. However, in the present case, the AP isotherms for temperatures in the close vicinity of the Curie point, T_C, acquire concave-upward curvature as $x \to x_c$. To elucidate this point further, the concave-upward curvature is completely absent in ap-$Ni_{76.1}$, starts showing up in ap-$Ni_{74.8}$ but the AP isotherms are linear above $(H/M) \cong 200$, and becomes pronounced in ap-$Ni_{74.3}$. In view of the finding, based on the electrical resistivity and EDAX data on ap-$Ni_{74.3}$ [18], that a minor isostructural phase of lower Ni

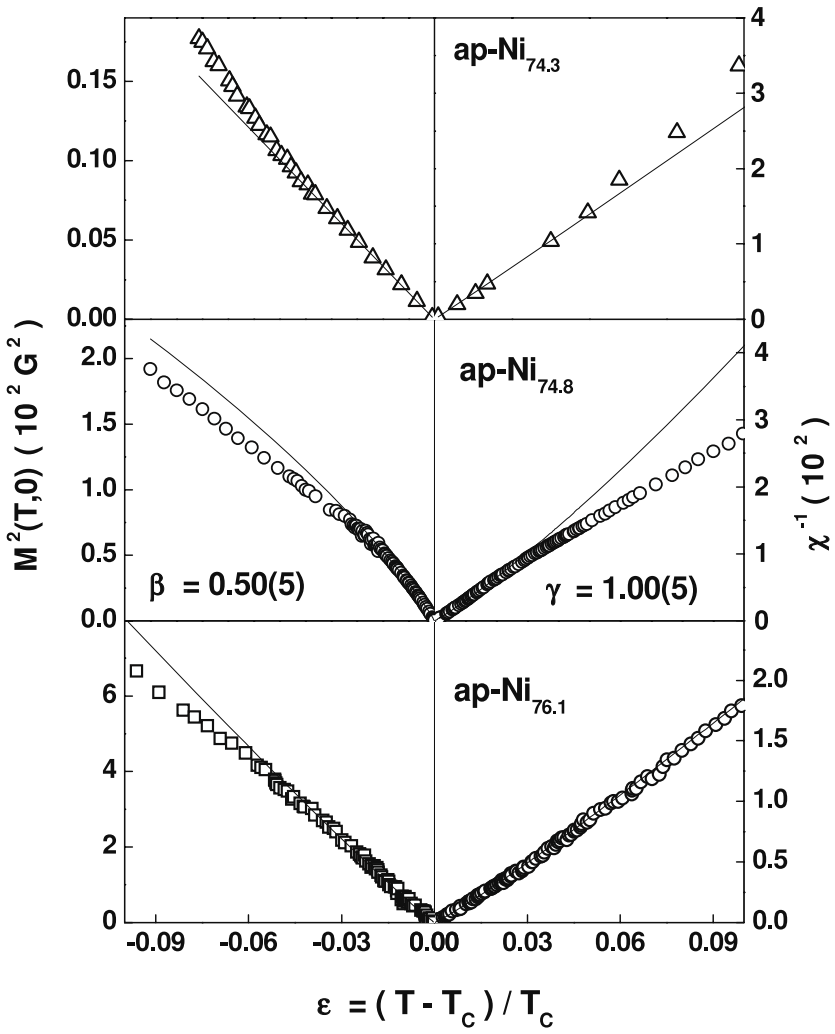

Figure 12. Spontaneous magnetization squared, $M^2(T, H = 0)$, and inverse initial susceptibility, $\chi^{-1}(T)$, as functions of the reduced temperature $\varepsilon = (T - T_C)/T_C$ within the range $-0.1 \leqslant \varepsilon \leqslant 0.1$. The continuous straight lines through the data (open symbols) represent the temperature variations of $M^2(T, H = 0)$ and $\chi^{-1}(T)$ predicted by equations (10) and (11) of the text in the asymptotic critical region when $\beta = 0.5$ and $\gamma = 1.0$.

concentration, and hence lower T_C, is present in this sample, such a departure from linearity basically reflects the presence of this additional magnetic phase. Taking cognizance of this result, extrapolations to $H = 0$ and $M^2 = 0$ of the *two linear regions* in the AP isotherms for ap-$Ni_{74.3}$, $(H/M) < 300$ (low-field (lf) region) and $(H/M) > 500$ (high-field (hf) region) have been carried out to obtain $M(T, 0) \equiv M(T, H = 0)$ and $\chi^{-1}(T)$ whereas the customary approach has been used for the remaining compositions. T_C marks the temperature at which the AP isotherm is *linear* over the entire H/M range and upon extrapolation passes through the origin, where both $M(T, 0)$ and $\chi^{-1}(T)$ go to zero. For ap-$Ni_{74.3}$, the low-field and high-field extrapolations yield the values for T_C as $T_C^{lf} = 48.25(5)$ K and $T_C^{hf} = 39.10(1)$ K, respectively, as indicated in figure 11(a). Note that the $M(T, 0)$ data (obtained from the Arrott plots and represented by crosses) have been used in figures 3, 6 and 8. The critical exponents β, γ and δ, defined as [24]

$$M(T, 0) = B(-\varepsilon)^{\beta} \qquad \varepsilon < 0 \tag{10}$$

$$\chi^{-1}(T) = \Gamma\varepsilon^{\gamma} \qquad \varepsilon > 0 \tag{11}$$

$$M(T = T_C, H) = AH^{1/\delta} \qquad \varepsilon = 0 \tag{12}$$

with $\varepsilon = (T - T_C)/T_C$, that characterize the asymptotic critical behaviour of spontaneous magnetization and initial susceptibility near the FM–PM phase transition, have been determined from the $M(T, 0)$, $\chi^{-1}(T)$ and $M(T = T_C, H)$ data using the method of analysis whose details are given elsewhere [24–26]. That the plots of $M^2(T, 0)$ against ε and $\chi^{-1}(T)$ against ε, based on equations (10) and (11) and shown in figure 12, are *linear* within the asymptotic critical region $-0.03 \leqslant \varepsilon \leqslant 0.03$ imply that the presently determined (mean-field) values for the critical exponents $\beta = 0.50(5)$ and $\gamma = 1.00(5)$ correctly describe the asymptotic critical behaviour of $M(T, 0)$ and $\chi^{-1}(T)$. However, larger than usual scatter in the $M(T, 0)$ and $\chi^{-1}(T)$ data precluded an unambiguous determination of the multiplicative logarithmic corrections to the mean-field power laws in the asymptotic critical region. Such corrections were previously reported [25, 26] for the alloy with stoichiometric composition, $Ni_{75}Al_{25}$, prepared in

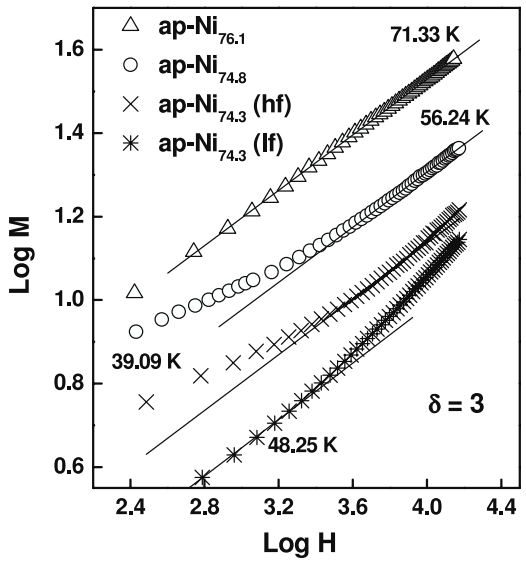

Figure 13. log M versus log H plots at $T = T_C$ for the samples ap-$Ni_{74.3}$, ap-$Ni_{74.8}$ and ap-$Ni_{76.1}$. The continuous straight lines through the data (symbols) represent the variations of log M with log H at $T = T_C$ predicted by equation (12) for the mean-field value $\delta = 3$.

different states of site disorder. Consistent with the mean-field values of the critical exponents β and γ, the log M–log H plots at $T = T_C$, based on equation (12) and shown in figure 13, yield the mean-field value $\delta = 3$ (inverse slope of the straight lines) for the critical exponent of the critical M–H isotherm in the *same magnetic field regimes* as those used for the extrapolation of the Arrott plot isotherms to $H = 0$ and $M^2 = 0$ in order to obtain $M(T, 0)$ and $\chi^{-1}(T)$. A comparison of the presently determined values for the critical exponent in samples with both compositional disorder and site disorder with those [25, 26] in the samples of stoichiometric composition but having different degree of site disorder permits us to conclude that both compositional disorder and site disorder have no effect on the critical behaviour of the weak itinerant-electron ferromagnets in question.

4. Summary

Magnetic behaviour of the binary Ni_xAl_{100-x} alloys with $x = 74.3$, 74.8, 75.1 and 76.1 at.% Ni, which possess both compositional disorder and site disorder, has been extensively studied over a wide temperature range that embraces the critical region near the ferromagnetic-to-paramagnetic phase transition. The results, so obtained, are compared with those reported in the literature on the ordered counterparts (which have only compositional disorder) and with the theoretical predictions, based on the spin-fluctuation models. Such a comparison reveals the following. (i) With increasing compositional disorder, i.e. as $x \to x_c$, Curie temperature, T_C, and spontaneous magnetization at 0 K, M_0, in the alloys with compositional disorder alone, decrease in accordance with the power laws $T_C(x) = t_x(x - x_c)^\tau$ and $M_0(x) = m_x(x - x_c)^\psi$. In the presence of site disorder, in addition to compositional disorder, these power laws still hold but with distinctly different values for the exponents τ and ψ, and a lower value (by nearly 1 at.% Ni) for the threshold Ni concentration, x_c. Compared to the values of T_C for the Ni_xAl_{100-x} alloys with compositional disorder alone, site disorder enhances T_C for a given composition (leaves T_C essentially unaltered) and this enhancement grows rapidly as $x \to x_c$ (for $x \geqslant 76$ at.%). Contrasted with this behaviour, except for $x \approx x_c$, M_0 is relatively *insensitive* to site disorder. Insensitivity of M_0 to site disorder basically reflects that site disorder has essentially no effect on the density of states, $N(E_F)$, at the Fermi level, E_F, and the shape of the density-of-states curve near E_F (except for $x \approx x_c$, where site disorder tends to primarily enhance $N(E_F)$ and thereby stabilize long-range ferromagnetic order for Ni concentrations below the threshold concentration, $x_c \cong$ 74.6 at.%, dictated by compositional disorder). As $x \to x_c$, site disorder increases the concentration of Ni atoms on the Al sub-lattice beyond that allowed by the compositional disorder and thereby enhances the number of Ni nearest neighbours for a given Ni atom and hence the T_C. (ii) At low and intermediate temperatures, spontaneous magnetization, $M(T, H = 0)$, as well as the 'in-field' magnetization, $M(T, H)$, exhibit *non-Fermi liquid* behaviour in the samples ap-$Ni_{74.3}$ and ap-$Ni_{74.8}$. As the critical concentration, x_c, is approached from above, i.e. as the *compositional disorder* increases, *stronger deviations* from the Fermi liquid behaviour occur and the temperature range over which the *non-Fermi liquid behaviour* persists *widens*. The non-Fermi liquid behaviour is taken to basically reflect that the increased compositional disorder *alters the spin-wave dispersion* at *finite* q such that, as q increases from $q = 0$, the spin-wave dispersion becomes increasingly similar to the non-propagating spin-fluctuation dispersion prevalent at temperatures close to T_C. In contrast, the ap-$Ni_{75.1}$ and ap-$Ni_{76.1}$ alloys follow the behaviour that the self-consistent spin-fluctuation theory [14] predicts for weak itinerant-electron ferromagnets without any disorder. That is (a) spin waves, at low temperatures ($T \leqslant 18$ K) and thermally excited (TE) plus zero-point (ZP) exchange-enhanced spin-density fluctuations, at intermediate temperatures and for temperatures close to T_C ($0.5T_C \leqslant T \leqslant 0.95T_C$), completely account for the observed temperature variations of $M(T, H = 0)$ and $M(T, H)$; (b) in accordance with the theoretical predictions [14, 19], the functional form for the suppression of spin waves and TE spin fluctuations by the magnetic field, H, is $\sqrt{H}$ for spin waves at low temperatures and $\sim H(\sqrt{H})$ for TE spin fluctuations at intermediate temperatures (temperatures close to T_C) and (c) compositional disorder and site disorder both leave these functional forms unaltered but reduce the spin-wave and (ZP + TE) spin-fluctuation 'stiffness' so that the suppression of these low-lying magnetic excitations by H becomes correspondingly large. (iii) For temperatures in the vicinity of T_C, $M^2(T, H = 0) \sim T^{4/3}$ and $M^2(T, H) \sim T^{4/3}$ for all the samples irrespective of the type of disorder present and regardless of the magnitude of field, provided $H < H_0$, the field required to quench the spin-fluctuation contribution to spontaneous magnetization. That these power law temperature variations are independent of H conforms well with the results of the self-consistent spin-fluctuation

calculations [14]. (iv) Both compositional disorder and site disorder have no effect on the critical behaviour of the alloys near the ferromagnetic-to-paramagnetic phase transition.

The observations similar to (ii)–(iv) stated above have also been made in paper I, based on the resistivity and magnetoresistance data taken on the same alloy compositions.

Acknowledgments

This work was supported by the Department of Science and Technology, India, under grants SP/S2/M-21/97 and SP/I2/MF-02-96-D. One of the authors (ACA) is grateful to the Council of Scientific and Industrial Research, India, for financial support.

References

[1] Kaul S N and Semwal A 2004 *J. Phys.: Condens. Matter* **16** 8695
[2] de Boer F R, Schinkel C J, Biesterbos J and Proost S 1969 *J. Appl. Phys.* **40** 1049
[3] de Chatel P F and de Boer F R 1970 *Physica* **48** 331
[4] Hambourger P D, Olwert R J and Chu C W 1975 *Phys. Rev.* B **11** 3501
[5] Buis N, Franse J J M and Brommer P E 1981 *Physica* B **106** 1
[6] Sasakura H, Suzuki K and Masuda Y 1984 *J. Phys. Soc. Japan* **53** 754
[7] Suzuki K and Masuda Y 1985 *J. Phys. Soc. Japan* **54** 630
[8] Dhar S K, Gschneidner K A Jr, Miller L L and Johnston D C 1989 *Phys. Rev.* B **40** 11488
[9] Yoshizawa M, Hirotaka S, Ikeda K, Okuno K, Saito M and Shigematsu K 1992 *J. Phys. Soc. Japan* **61** 3313
[10] Semwal A and Kaul S N 2004 *J. Phys.: Condens. Matter* **16** 8675
[11] Semwal A and Kaul S N 1999 *Phys. Rev.* B **60** 12799
[12] Moriya T and Kawabata A 1973 *J. Phys. Soc. Japan* **34** 639
Moriya T and Kawabata A 1973 *J. Phys. Soc. Japan* **35** 669
Moriya T 1985 *Spin fluctuations in Itinerant Electron Magnetism* (*Springer Series in Solid State Sciences* vol 56) (Berlin: Springer) and references cited therein
[13] Lonzarich G G and Taillefer L 1985 *J. Phys. C: Solid State Phys.* **18** 4339
[14] Kaul S N 1999 *J. Phys.: Condens. Matter* **11** 7597
[15] Aharony A, Alexander S, Entin-Wohlman O and Orbach R 1985 *Phys. Rev.* B **31** 2565
Aharony A, Entin-Wohlman O, Alexander S and Orbach R 1987 *Phil. Mag.* B **56** 949
[16] Nakayama T, Yakubo K and Orbach R 1994 *Rev. Mod. Phys.* **66** 381 and references cited therein
[17] Kaul S N and Srinath S 2001 *Phys. Rev.* B **63** 094410
[18] Abhyankar A C and Kaul S N 2008 *J. Phys.: Condens. Matter* **20** 445227
[19] Kaul S N 2005 *J. Phys.: Condens. Matter* **17** 5595
[20] Bernhoeft N R, Lonzarich G G, Mitchell P W and MckPaul D 1983 *Phys. Rev.* B **28** 422
[21] Sedameni F, Roessli B, Böni P, Vorderwish P and Chatterji T 2000 *Phys. Rev.* B **62** 1083
[22] Lonzarich G G 1997 *The Electron* ed M Springford (New York: Cambridge University Press) chapter 6
[23] Stewart G R 2001 *Rev. Mod. Phys.* **73** 797
[24] Kaul S N 1985 *J. Magn. Magn. Mater.* **53** 5
[25] Semwal A and Kaul S N 2001 *Phys. Rev.* B **64** 014417
[26] Semwal A and Kaul S N 2002 *J. Phys.: Condens. Matter* **14** 5829